Surface Science 230 (1990) 27–34
North-Holland

SURFACE STRUCTURE STUDIES OF Cl ADSORPTION ON Ag{001} USING ENERGETIC ION BEAMS

Che-Chen CHANG * and N. WINOGRAD

Department of Chemistry, The Pennsylvania State University, 152 Davey Laboratory, University Park, PA 16802, USA

Received 28 September 1989; accepted for publication 28 November 1989

Angle-resolved SIMS experiments have been employed to study the bonding geometry of Cl on Ag{001}. The procedure was to bombard the target with 2 or 3 keV Ar^+ ions in the low dose mode at various incident angles and to measure the desorption of Ag^+ or Cl^- ions at various detection angles. For the case of the c(2 × 2)-Cl/Ag{001} structure, azimuthal angle distributions of both Ag^+ and Cl^- ions indicate that the Cl atom binds in the four-fold hollow site. Measurement of the polar angle distributions suggests that the Cl overlayer is above the surface plane, ruling out the formation of an epitaxial AgCl layer. The Ag–Cl bond-length was determined to be 2.60 ± 0.04 Å using shadow-cone enhanced desorption. With this measurement the angle of incidence of the ion beam is varied until the shadow-cone created by a target Cl atom intersects a nearby Ag atom. The result is in agreement with earlier LEED experiments.

1. Introduction

The determination of the structure and reactivity of halogens with transition metal surfaces is a problem of longstanding interest. These systems are particularly important in furthering our understanding of the surface chemical bond. Depending upon the specific halide, metal, temperature and surface coverage the resulting chemisorbed overlayer may exhibit highly ionic or covalent characteristics [1]. Further, since the halide adsorbate may possess significant electronic charge, it is also an important probe for examining adsorbate–adsorbate interactions [2–4]. From a more practical viewpoint, the halide/metal combination is important as an additive for heterogeneous catalytic reactions [5] and in dry-etching of electronic materials [6].

In this paper we focus on the interaction of Cl_2 with Ag{001} at room temperature. This simple model system has presented many challenges to researchers over the years. Although the low energy electron diffraction (LEED) pattern clearly reveals a sharp c(2 × 2) symmetry after 5 L exposure of Cl_2, controversies have persisted regarding the structure of this layer. An early model known as the mixed layer model (MLM) suggests that an epitaxial layer of AgCl is formed directly on top of the Ag{001} surface [7]. Later, extensive LEED analysis showed that the Cl atom was bound to the four-fold hollow site of the Ag{001} surface and that the Ag–Cl bond-length was 2.61 Å [8]. This result for this simple overlayer model (SOM) was later confirmed using surface extended X-ray absorption fine-structure (SEXAFS) [9]. This technique indicated that the adsorbed Cl atom had only 4 nearest-neighbors with a Ag–Cl bond-length of 2.69 ± 0.03 Å and ruled out the MLM configuration. Both of these structures are shown schematically in fig. 1. The picture becomes more complicated as the coverage of Cl is increased further or when the temperature is changed. For example, evidence for a SOM → MLM transition starting at ~ 430 K has been reported [10], but few structural details are yet available. There have been virtually no attempts to examine the diffusion of Cl into the bulk of the crystal or to examine the influence of possible sub-surface Cl on the surface properties. The answer to many of these questions are presently

* Present address: Department of Chemistry, University of Hawaii, 2545 The Mall, Honolulu, HI 96822, USA.

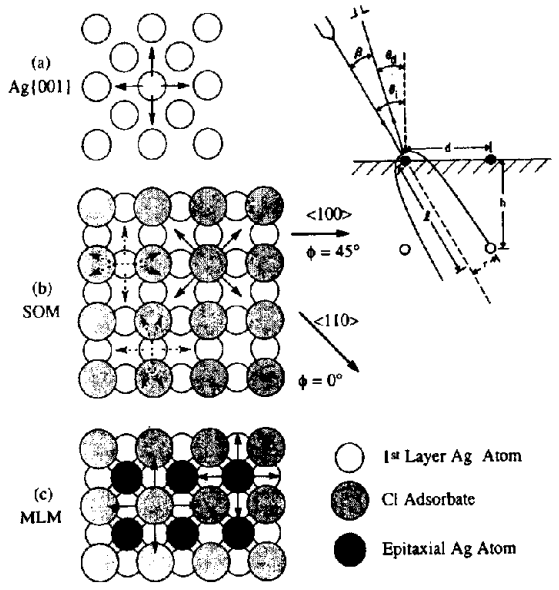

Fig. 1. Schematic picture of (a) Ag{001}, (b) the simple-overlayer-model (SOM) of c(2×2)-Cl/Ag{001} and (c) the mixed-layer-model (MLM) of c(2×2)-Cl/Ag{001}. The definitions of the angles used in this work are noted in the upper right. The angle θ_i is the angle of incidence of the ion beam, θ_d is the detector angle and β is the difference between the two. Note also that the shadow-cone is represented by a radius r at a distance l behind the target atom.

beyond the capability of most surface science techniques to solve them:

In a recent series of articles, we have reported on the use of angle-resolved secondary ion mass spectrometry (SIMS) experiments aimed toward elucidation of the structure of Cl overlayers on a variety of crystal faces of Ag [2–4]. These experiments involve bombardment of the crystal with a keV Ar^+ ion at a specific angle followed by measurement of the intensity of desorbed ions at various azimuthal and polar angles. There are several aspects to these studies. First, the presence of the Cl overlayer greatly enhances the probability of desorbing secondary ions, allowing measurements with very high sensitivity. Second, using accurate molecular dynamics computer simulations we have found two important energy-deposition mechanisms for these crystalline systems which lead to secondary ions [11]. Normally, the desorbing particle is given its kinetic energy by interacting with atoms that are in motion below the surface. Collisions of these atoms with a surface atom forces desorption to be channeled in specific directions and blocked in specific directions by other surface atoms [12]. The ion intensity along these channeling and blocking directions obtained by azimuthally rotating the crystal allows a simple determination of the bonding geometry of the adsorbate atom. In addition, we have found that by changing the polar angle of incidence of the primary ion beam we can determine the angle at which the shadow-cone of the target atom intersects a nearby atom [3,4,11,13]. Using this angle, the known bonding site geometry of the adsorbate, and the known shadow-cone shape, it is possible to extract an accurate value for the adsorbate–surface bond-length.

In this paper, we present an initial study of the c(2 × 2)-Cl overlayer on Ag{001} obtained at room temperature. For this study, we take advantage of the channeling and blocking concepts to determine the adsorption site of the Cl and the shadow-cone experiments to find the Ag–Cl bond-length. The results show that Cl adsorbs into the four-fold hollow site with a Ag–Cl bond-length of 2.60 ± 0.04 Å, in agreement with the LEED experiments and in near agreement with SEXAFS. We also show that there are no Ag atoms in the plane of the Cl overlayer, unequivocally ruling out the MLM structure. These results, although confirming other experimental data or conclusions, are important since they further establish the validity of our techniques and provide an important base of information to begin studies of the Cl/Ag system under much more complex conditions.

2. Experimental aspects

All experiments were performed in a UHV angle-resolved scattering chamber that has been described in detail elsewhere [14]. Briefly, the chamber is equipped with a stationary differentially pumped Riber CI50 noble gas ion source, LEED, and auger electron spectroscopy (AES). The mass detector is a Riber AQX 156 quadrupole mass filter equipped with a 90° electrostatic sector for energy selection of desorbed ions. This detec-

tor is mounted on a 22″ flange which is moveable through 180° so that the angle between the ion source and detector can be continuously varied. The rotation occurs about two differentially pumped teflon seals. The pressure in the chamber is $\sim 2 \times 10^{-10}$ Torr during rotation of the detector. Using this configuration, the angular resolution is about $\pm 0.5°$ in the polar direction and $\pm 2°$ in the azimuthal direction, depending of course on the absolute values. The angle values themselves were determined to $\pm 0.5°$.

The Ag single crystal was oriented along the {001} direction to $\pm 0.5°$ using Laue diffraction. The crystal was mechanically polished to optical quality before mounting in the sample holder. The surface was then cleaned in-situ by cycles of heating and Ar^+ ion bombardment (2 keV, 0.5 μA cm^{-2}). The surface was considered clean when no adventitious carbon, oxygen or chlorine could be observed by AES and the Ag^+ SIMS signal reached a minimum value. Typical contaminants observed in the SIMS spectra after cleaning include Na^+, Al^+, K^+ and Cl^- ions. The intensity of these ions is not believed to be significant since the SIMS technique is known to be extremely sensitive to their presence. The LEED apparatus was used to ensure the presence of (1×1) surface order.

Orientation of the sample surface with respect to the ion beam was controlled by a goniometer which allows independent rotation of the crystal to any azimuthal angle, and a polar rotation to vary the ion beam incident angle. Our angle conventions are shown in fig. 1. The detector is positioned at $\theta_d = \theta_i - \beta$. A negative value of θ_i indicates that when both the ion source and the detector are on the same side of the surface normal, the ion source is positioned closer to the surface normal than the detector.

Atomic chlorine was deposited on the surface by exposing the crystal to Cl_2 at room temperature. Exposures are reported using an uncorrected pressure reading from a nude Bayard-Alpert ionization gauge. The resulting ion beam experiments were performed in the static mode. Typically, a 2 or 3 keV Ar^+ ion beam with an incident current of 2 nA and a cross section of 2 mm^2 was used to record the angular measurements. All angle-resolved spectra were repeated after annealing and redosing to ensure that the results were not being influenced by beam damage.

3. Results and discussion

The strategy for determination of adsorbate structures is to initially determine the bonding geometry of the overlayer using channeling and blocking schemes and then to subsequently evaluate bond-lengths using shadow-cone-enhanced desorption. For the specific case considered here, an overlayer structure exhibiting a sharp $c(2 \times 2)$ LEED pattern was prepared by exposure of a cleaned Ag{001} crystal to 5.0 L of Cl_2 at room temperature. The crystal was then bombardment with 2 or 3 keV Ar^+ ions. The intensity of the desorbed Ag^+ or Cl^- ions was monitored as a function of the azimuthal angle, ϕ, at various values of θ_d and θ_i. We select only those desorbed ions whose kinetic energy is greater than 20 eV since these particles leave the surface early in the collision cascade and before nearby surface atomic rearrangement has occurred [12]. Moreover, the image potential between the ejecting ion and its image charge in the substrate and the coulomb potential among adsorbates will not significantly alter the trajectory of high kinetic energy ions [15].

3.1. Azimuthal and polar angles distributions at $\theta_i = 0°$.

It is straightforward to determine the bonding configuration of $c(2 \times 2)$-Cl on Ag{001} by a brief inspection of the azimuthal angle data and from the structural features evident from fig. 1. For the SOM, the Cl atoms are bound to the four-fold hollow sites. The bond-angle between the surface normal and the line connecting a surface Ag atom and a Cl adsorbate, given reasonable values of estimated interatomic spacings, is $\sim 50°$. For the MLM, of course, this angle is close to 90°. From channeling and blocking arguments [12,15,16], we expect the clean Ag{001} surface to exhibit Ag^+ ion maxima along ⟨100⟩ azimuths and minima along ⟨110⟩ azimuths at virtually all values of θ_d. For the $c(2 \times 2)$-Cl/Ag{001} SOM structure,

however, the presence of the Cl atoms should strongly block desorption of Ag^+ ions along two of the four ⟨100⟩ directions at θ_d near 45° and more weakly block this desorption at other values of θ_d. For the MLM structure the channeling directions remain along ⟨100⟩ and the blocking directions remain along ⟨110⟩, regardless of the value of θ_d. These effects are shown schematically in figs. 1b and 1c.

The experimental results of the important Ag^+ ion azimuthal angle scans are shown in fig. 2, for the c(2 × 2)-Cl/Ag{001} structure. In all cases, we observe nearly perfect four-fold symmetry as required in LEED. At $\theta = 45°$, the pattern as shown in fig. 2b resembles that observed for the clean surface. According to the reasoning discussed above, this behavior is consistent with either the SOM or the MLM structure. At $\theta_d = 60°$ (fig. 2a) or $\theta_d = 30°$ (fig. 2c), however, the CL overlayer atom is observed to distort the trajectory of the departing Ag^+ ion by $\sim \pm 20°$ away from the ⟨100⟩ azimuths. This effect is shown schematically by the split dotted arrows in fig. 1b. Although the symmetry of these two patterns is similar, the

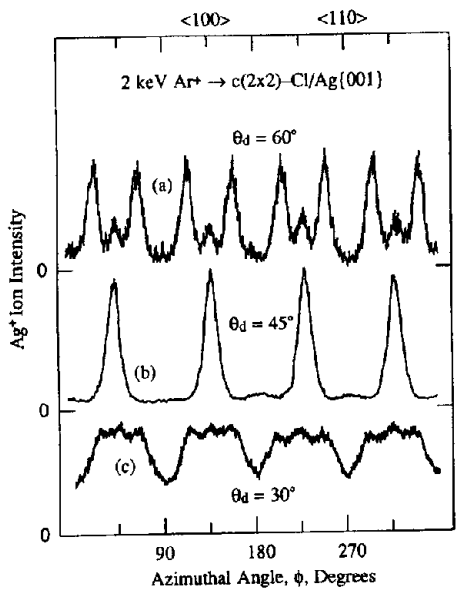

Fig. 2. Azimuthal angle distributions of 20 ± 3 eV Ag^+ ions desorbed from c(2×2)-Cl/Ag{001} after bombardment at $\theta_i = 0°$ with 2 keV Ar^+ ions at (a) $\theta_d = 60°$, (b) $\theta_d = 45°$ and (c) $\theta_d = 30°$. The relative intensities of each set of curves are *not* directly comparable, but may be estimated from fig. 4.

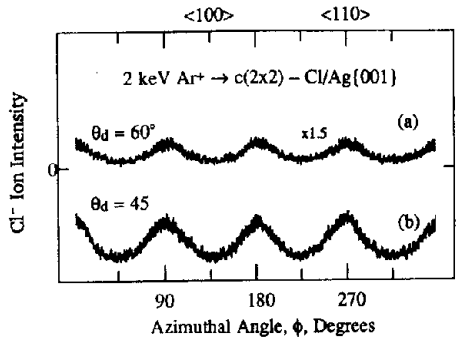

Fig. 3. Azimuthal angle distributions of 20 ± 3 eV Cl^- ions desorbed from c(2×2)-Cl/Ag{001} after bombardment at $\theta_i = 0°$ with 2 keV Ar^+ ions at (a) $\theta_d = 60°$ and (b) $\theta_d = 45°$.

relative intensity of the new features is quite different. Without more detailed calculations, however, we are reluctant to put added significance to these differences. Note that the structure seen in figs. 2a or 2c is not only inconsistent with the MLM but also with other bonding geometries such as the a-top or two-fold bridge configurations.

Although these results by themselves are strongly indicative of the Cl bonding configuration, there are many other experimental configurations we can examine to further confirm our hypothesis. The Cl^- ion azimuthal angle anisotropies are shown in fig. 3. For these ions, the yield maxima occur along ⟨110⟩ and the yield minima occur along ⟨100⟩ for all values of θ_d. As seen by inspecting the channeling directions denoted by the arrows associated with the Cl atoms in fig. 1, this result is only expected for the SOM.

The relative behavior of the Cl^- ion intensity and the Ag^+ ion intensity as a function of θ_d is also quite instructive. As shown in fig. 4, the Ag^+ ion intensity along ⟨100⟩ is low near detection angles close to the surface normal, and reaches a maximum at $\theta_d = 48°$. The Cl^- ion yield, however, is highest at small values of θ_d, decreasing continuously to near zero at $\theta_d > 70°$. These effects suggest that the Cl atoms reside above the Ag atoms and not in a co-planar configuration. If Ag and Cl were coplanar as for the MLM, the θ_d distributions would be expected to be similar.

We have performed a limited series of azimuthal angle measurements at lower Cl coverages to ex-

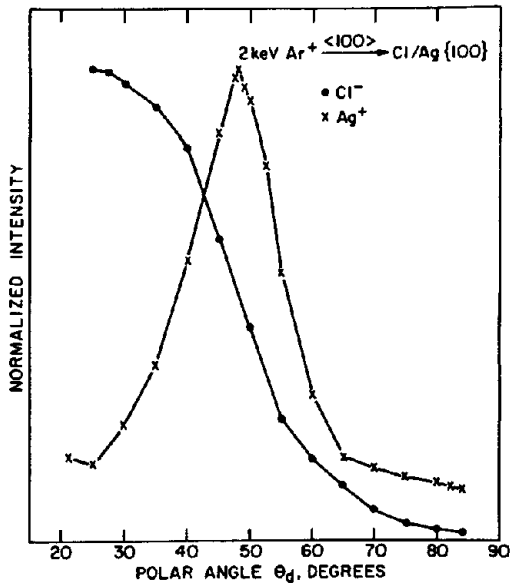

Fig. 4. Polar angle distributions of Ag^+ and Cl^- ions for c(2×2)-Cl/Ag{001} after bombardment at $\theta_i = 0°$ with 2 keV Ar^+ ions.

amine the influence of overlayer scattering on the observed angular anisotropies. The Ag^+ ion azimuthal scans obtained after 1.5 L Cl_2 exposure at $\theta_d = 30°$ and 45° are seen in figs. 5a and 5b, respectively. The influence of Cl overlayer scattering is not evident at the lower coverages when comparing fig. 2b and fig. 5a due to symmetry considerations. When comparing fig. 2c and fig. 5b, however, it is clear that at the lower coverages,

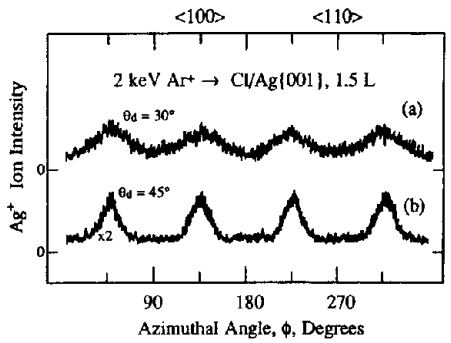

Fig. 5. Azimuthal angle distributions of 20±3 eV Ag^+ ions desorbed from Ag{001} exposed to 1.5 L Cl_2, and bombarded at $\theta_i = 0°$ with 2 keV Ar^+ ions at (a) $\theta_d = 30°$ and (b) $\theta_d = 45°$.

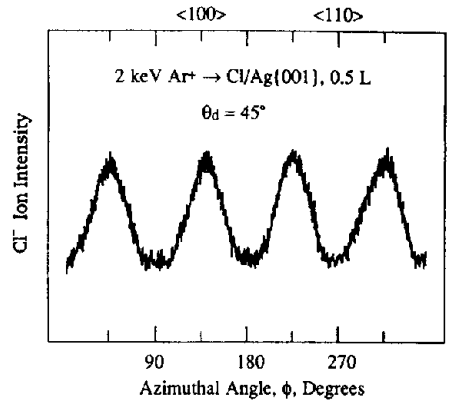

Fig. 6. Azimuthal angle distributions of 20±3 eV Cl^- ions desorbed from Ag{001} exposed to 0.5 L Cl_2, and bombarded at $\theta_i = 0°$ with 2 keV Ar^+ ions at $\theta_d = 45°$.

the structure ascribed to Cl blocking at ±20° of ⟨100⟩ is significantly reduced.

Finally, in fig. 6, we show the Cl^- azimuthal angle distributions at $\theta_d = 45°$ obtained at a Cl_2 exposure of only 0.5 L. Interestingly, the maximum intensities are now observed to be shifted by precisely 90° from ⟨110⟩ to ⟨100⟩ as seen by comparing to fig. 3b. Although we have not performed molecular dynamics simulations to determine the origin of this effect, we believe it almost certainly arises from the lack of overlayer scattering effects. At low coverages, and at $\theta_d =$ 45°, the Cl atom is directly in the path of a desorbing Ag atom. Its bonding location is also higher above the surface than other cases we have considered in the past [16]. Surface channeling by other Ag atoms is apparently not as significant as the direct collisions between these desorbing Ag atoms and the Cl adsorbate. At higher exposures, however, there are open channels in the Cl overlayer and desorption of Cl^- ions is preferred along ⟨110⟩.

At this point, then, the azimuthal angle data, the polar angle data, and the behavior at different Cl coverages all strongly point toward the SOM. Many of our experiments are, in fact, totally inconsistent with other bonding configurations including the MLM, a-top and two-fold bonding geometries. With the adsorption site known from our experiments, it remains only to determine the

bond-lengths using shadow-cone enhanced desorption.

3.2. Shadow-cone enhanced desorption

The Cl^- ion yield as a function of θ_i is shown in fig. 7 and a similar plot for the Ag^+ ion yield is shown in fig. 8. The data are reported for several values of β, the angle between the incident beam and the detector. As we have shown from an extensive study of Ag{110} [11] and Cl adsorbed on Ag{110} [3,4], the maxima in these yields are generally produced when the shadow-cone created by the target atom intersects the nuclear position of a nearby atom. This energy focusing induces extensive action in the near-surface region which enhances the overall desorption yield. There are two important geometries which contribute strongly to the enhancement, which we call the F_1 mechanism and the F_{2A} mechanism illustrated in fig. 9. The F_1 mechanism involves intersection of the shadow-cone edge with another top-layer atom while the F_{2A} mechanism involves intersection of the shadow-cone edge with a second-layer atom. Note that in both cases, the forward-edge of the shadow-cone is involved in the collision mechanism. Although events involving the back-edge of the shadow-cone can contribute to the yield, we have found that these processes are not as effective at enhancing the desorption of ions. At the relatively small values of θ_d used in these experiments, the intensity resulting from F_{2A} processes is found to be much larger than those resulting from F_1 processes.

In fig. 7, there are two pronounced yield maxima observed at the critical angles $\theta_{ic} = 28°$ and

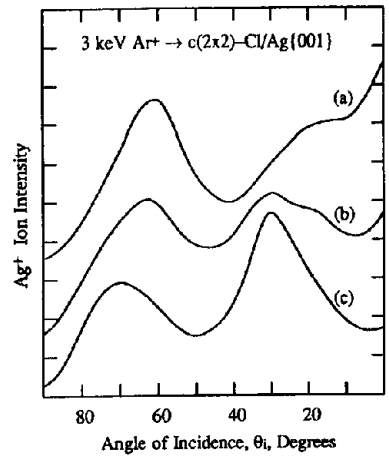

Fig. 8. Variation of Ag^+ ion yield as a function of θ_i for c(2×2)-Cl/Ag{001} bombarded by 3 keV Ar^+ ions. The angle between the detector and the incident ion beam, β, is (a) 25°, (b) 35° and (c) 45°. The crystal is aligned along ⟨100⟩.

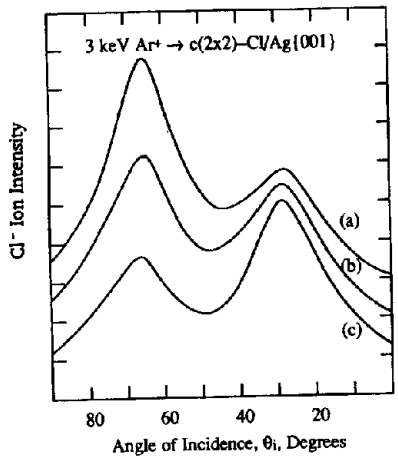

Fig. 7. Variation of Cl^- ion yield as a function of θ_i for c(2×2)-Cl/Ag{001} bombarded by 3 keV Ar^+ ions. The angle between the detector and the incident ion beam, β, is (a) 25°, (b) 35° and (c) 45°. The crystal is aligned along ⟨100⟩.

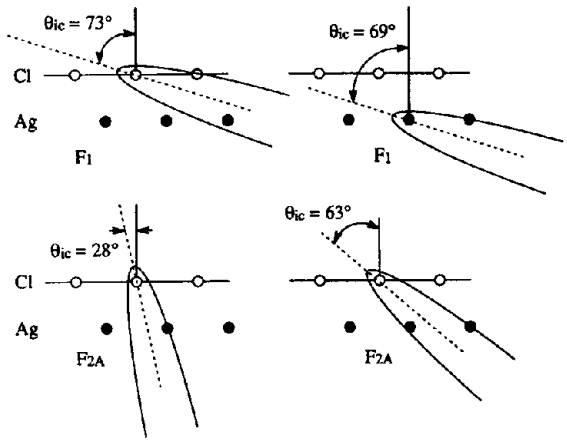

Fig. 9. Schematic representations of possible mechanisms which result in the observed secondary ion yield enhancement. The values of θ_{ic} are calculated using a Ag–Cl bond-length of 2.60 Å.

64°, respectively. It is possible to calculate the Ag–Cl bond-length from these data. The shadow-cone shape has been shown to be accurately represented using a Thomas–Fermi–Molière potential [17,18]. The Firsov screening factor may be determined with no free parameters from the empirical relation [19]

$$f(Z_1, Z_2) = 0.69 + 0.0051(Z_1 + Z_2), \qquad (1)$$

where Z_1 is the atomic number of the primary particle and Z_2 is the atomic number of the target atom. For Ar → Cl, $f(18, 17) = 0.87$ and for Ar → Ag, $f(18, 47) = 1.02$. Established procedures may be used to obtain the shadow-cone radius, r, as a function of the distance, l, behind the shadowing atom [20]. From the intensity and position of the yield maximum, the $\theta_{ic} = 28°$ peak may be ascribed to an F_{2A} mechanism as illustrated in fig. 9. Along the ⟨100⟩ direction of the c(2 × 2)-Cl/Ag{001} overlayer, d is assumed to be equal to the bulk spacing of 2.043 Å, yielding a unique value of $h = 1.61 \pm 0.04$ Å. From trigonometry the Ag–Cl bond length is calculated to be 2.60 Å. The two primary assumptions in this calculation are (i) that the Cl atom is bound to the four-fold hollow site and (ii) that the Ag–Ag spacing in the first layer is not altered by th chemisorption process.

The second yield maximum at $\theta_{ic} = 64°$ is a bit more complicated to interpret quantitatively. As shown in fig. 9, there are two possible F_1-type mechanisms which could be observed corresponding to intersections involving Ag shadow-cones or Cl shadow-cones. Using $d = 4.086$ Å, the θ_{ic} values should be seen at 69° and 73°, respectively. These numbers are significantly different than observed experimentally. Moreover, previous studies suggest that the Cl atom should sufficiently block the Ag atom from the primary beam so as to effectively attenuate the F_1 mechanism [3]. Finally, we would expect the intensity of the F_1 mechanism to be much weaker than the F_{2A} mechanism at small values of θ_d even without Cl blocking as found on Ag {110} [11]. The characteristics of this peak, then, are not consistent with an F_1 assignment.

It is possible that the $\theta_{ic} = 64°$ peak is associated with an F_{2A} mechanism involving a target Cl atom and a Ag atom located below the Cl atom and displaced laterally by 6.129 Å. This rather long-range mechanism is illustrated in fig. 9. The yield resulting from the interaction might be expected to be large since a second-layer atom is involved in the process. We have not yet performed any molecular dynamics calculations to check the validity of this hypothesis. This peak position, however, would correspond to a Ag–Cl bond-length of 2.51 Å. We are reluctant to place quantitative significance on this value since the target Cl atom and the important Ag atom are far apart, leaving our simple analysis subject to errors arising from distortions of the shadow-cone.

Finally, with respect to fig. 7, note that the position of the yield maxima is completely independent of the value of β, although the relative intensities change somewhat. This behavior is expected if the trajectory of the desorbing atom, i.e. Cl, is not altered systematically by overlayer atoms. This β independence, then, is indicative of the fact that the Cl^- ions arise solely from the top atomic layer, as expected for the SOM geometry. Thus, the two features of fig. 7 are both assigned to F_{2A} mechanisms with the $\theta_{ic} = 28°$ peak yielding a Ag–Cl bond-length of 2.60 ± 0.04 Å.

There is an important piece of information to be gleaned from the Ag^+ ion yield as a function of θ_i as shown in fig. 8. Although the double-peaked structure found for the Cl^- ion yield curves is evident, there are a number of obvious differences. The positions of the maxima are clearly not independent of β and new features are visible. The β dependence of the θ_i distributions provides convincing evidence that there are atoms above the plane of surface Ag atoms which can alter the direction of desorbing ions. This blocking effect results in the observed new features and is particularly noticeable at $\theta_i = 0°$ and $\beta = 45°$ as seen in curve c of fig. 8. There is an open channel at an angle of 45° with respect to the normal along the ⟨100⟩ azimuth of Ag{001}. The Cl atoms which bind in four-fold hollow sites cover 50% of these channels in the c(2 × 2) surface structure. Those Ag atoms which desorb along this channel will be affected most strongly at this incident beam/detector geometry, as observed. We would expect the shape of the yield curves in fig. 7 and fig. 8 to be identical for the MLM.

4. Conclusions and prospects

We have utilized angle-resolved SIMS in a number of different modes to elucidate the structure of c(2 × 2)-Cl/Ag{001}. From azimuthal angle data it is possible to determine the geometry of the adsorption site of the Cl adsorbate and to distinguish between the SOM and the MLM. From shadow-cone enhanced desorption experiments for Cl^- ions, it is possible to determine the Ag–Cl bond-length. For polar angle studies and from evaluation of the β dependence of the secondary ion yield, it is possible to determine whether the adsorbate is above or below the plane of first-layer atoms. These set of experiments, then, provide a rather complete strategy for examining the surface structure of simple model systems.

With this methodology under control for the well-characterized c(2 × 2)-Cl/Ag{001} case, it is of interest to examine the structure of Cl adsorbates under a variety of different circumstances. We have already taken advantage of the high sensitivity of the shadow-cone enhanced desorption experiments to detect a significant 0.4 Å expansion of the Ag–Cl bond on Ag{110} in the limit of zero coverage to a bond-length of 2.90 Å [3,4]. This result suggests that the isolated Cl adatom initially adsorbs in an ionic configuration, but rapidly forms a more covalent-type of bond at higher coverages. This idea also appears to apply to the case considered here, as the reported Ag–Cl bond-length of 2.60 Å on Ag{001} compares favorably with the value of 2.56 Å found on Ag{110} [4,21]. No low-coverage experiments have yet been reported on Ag{001}. Finally, the flexibility of the angle-resolved SIMS experiments opens the possibility of examining the structural changes which occur between the formation of the SOM and bulk AgCl. There have been indications that there is a phase transition at ~ 430°C associated with SOM → MLM [10]. Our approach has been successful at directly monitoring this transition by measuring the changes in ϕ, θ_d θ_i and β as a function of temperature [22].

Acknowledgment

The authors wish to thank The Petroleum Research Foundation, administered by the American Chemical Society, the National Science Foundation and the Office of Naval Research for partial financial support.

References

[1] K.K. Kleinherbers, E. Janssen, A. Goldmann and H. Saalfeld, Surf. Sci. 215 (1989) 394.
[2] D.W. Moon, R.J. Bleiler and N. Winograd, J. Chem. Phys. 85 (1986) 1097.
[3] C.-C. Chang, G.P. Malafsky and N. Winograd, J. Vac. Sci. Technol. A 5 (1987) 981.
[4] N. Winograd and C.-C. Chang, Phys. Rev. Lett. 62 (1989) 2568.
[5] N. Sato and M. Seo, J. Catal. 24 (1972) 224.
[6] T.J. Chuang, Surf. Sci. 178 (1986) 763.
[7] G. Rovida and F. Pratesi, Surf. Sci. 51 (1975) 270.
[8] F. Jona and P.M. Marcus, Phys. Rev. Lett. 50 (1983) 1823.
[9] G.M. Lamble, R.S. Brooks, J.-C. Campuzano and D.A. King, Phys. Rev. B 36 (1987) 1796.
[10] M. Kitson and R.M. Lambert, Surf. Sci. 100 (1980) 368.
[11] C.-C. Chang and N. Winograd, Phys. Rev. B 39 (1989) 3467.
[12] N. Winograd, Prog. Solid State Chem. 13 (1982) 285.
[13] R. Blumenthal, S.K. Donner, J.L. Herman, R. Trehan, K.P. Caffey, B.D. Weaver, E. Furman and N. Winograd, J. Vac. Sci. Technol. B 6 (1988) 1444.
[14] R.A. Gibbs and N. Winograd, Rev. Sci. Instrum. 52 (1981) 1148.
[15] R.A. Gibbs, S.P. Holland, K.E. Foley, B.J. Garrison and N. Winograd, Phys. Rev. B 24 (1981) 6178.
[16] S.P. Holland, B.J. Garrison and N. Winograd, Phys. Rev. Lett. 43 (1979) 220.
[17] I.M. Torrens, Interatomic Potentials (Academic Press, New York, 1972).
[18] T.M. Buck, I. Stensgaard, G.H. Wheatley and L. Marchut, Nucl. Instrum. Methods 170 (1980) 519.
[19] D.J. O'Conner and R.J. MacDonald, Radiat. Eff. 34 (1977) 247.
[20] J.A. Yarmoff, D.M. Cyr, J.H. Huang, S. Kim and R.S. Williams, Phys. Rev. B 33 (1986) 3856.
[21] D.J. Holmes, N. Panagiotides, C.J. Barnes, R. Dus, D. Norman, G.M. Lamble, F. Della Valle and D.A. King, J. Vac. Sci. Technol. A 5 (1987) 703.
[22] C.-C. Chang and N. Winograd, manuscript in preparation.